



# Fabrication and characterization of PSi/nanometal hybrid structures by laser for CO gas sensor

Amer Badr Dheyab<sup>1</sup> · Safaa Idan Mohammed<sup>1</sup> · Marwa Kamal Mustafa<sup>1</sup> · Rasha Saad Fayadh<sup>1</sup> · Noor Luay Hussein<sup>1</sup>

Received: 4 September 2019 / Accepted: 28 January 2020 / Published online: 11 February 2020  
© Islamic Azad University 2020

## Abstract

Mesoporous silicon (mesoPSi) layers fabricated by the photoelectrochemical etching (PECE) method in hydrofluoric acid (HF) are active as carbon monoxide gas sensors. The modified porous silicon (PSi) can be used with noble metals to manufacture an effective gas sensor. Embedded gold, platinum, and palladium nanoparticles Au, Pt, and Pd-NPs could modify the surface morphology of mesoPSi and form mesoPSi/AuPtPd-NPs hybrid structures through a simple and dipping process in fixed salt concentrations. The morphology of the hybrid structures has been studied using scanning electron microscopy and X-ray diffraction. The prepared gas sensor has measured the electrical characteristics at room temperature. Shape, nanoparticle size, and specific surface area strongly influenced the current–voltage characteristics. The results show that Au, Pd, and Pt-NPs sizes prepared by the dipping process for mesopore-like structures were in the range from 0.64 to 7.53 nm. Besides, considerable improvements in the response, recovery times and sensitivity of gas sensor were noticed when decreasing the incorporated Au, Pd, and Pt-NPs to the mesoPSi matrix.

**Keywords** MesoPSi · SEM · Gas sensing · Photoelectrochemical · AuPtPd-NPs hybrid structures

## Introduction

Porous silicon (PSi) is a new material of importance due to its morphological properties. The PSi performs like a heatproof in the application of a heating plate [1]. The main advantage of PSi gas sensor is the low consumption of power and the short transient thermal times called ‘passive processes.’ This makes PSi material suitable for thermally insulated microheat due to its large surface area. The PSi layer can be approximately a quick and excellent etching method. Besides, the PSi layer acts like the gas detection device with optical, electrical or thermal measurements. PSi gas sensitive is considered simple and of low cost, and it relies on resistance. It can be of high sensitivity and called a sensor of active processes or active sensor [2].

The gas-detecting devices are considered ideal, and there are some points to be taken into account [3]:

- The lowest value of gas in the laboratory can be sensed or identified through what is called ‘sensor.’
- The capability of gas sensors in identifying a precise gas between gas combinations is defined as selectivity.
- The interval of the time when the gas concentration spreads has a precise value to this sensor by producing a warning signal that it is the response time.
- Returning the sensor to its initial detection status later is defined as reversibility.
- Stability.

Modification of the PSi layer was found by combining the constituent nanomaterial and the metal oxide layer as an effective means of improving the gas sensor performance [4]. In these studies, the PSi aspects of the substrate were covered with a thin layer of gold. The resulting room temperature devices were extra sensitive to the voltage used in the CO<sub>2</sub> gas; the nanostructured PSi had a greater response than other similar sensors. The performance of nanosilicon wires was studied; it was modified using nanoparticles of gold and platinum, as CO<sub>2</sub> gas sensors. A strong dependence was found on the type of metallic nanoparticle [5]. Whether loading using Pt, Pd, and thin SnO<sub>2</sub> films could improve their ability to detect unused sensors was investigated [6].

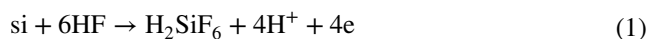
✉ Safaa Idan Mohammed  
safaadali431@gmail.com

<sup>1</sup> Ministry of Science and Technology, Baghdad, Iraq

The metal oxide gas sensors were formed in discharge on the basis of exposure to gas. Platinum and palladium were anesthetized by indium oxide gas, and their performance was compared to the concentration of oxygen [7]. The Platinum modifying palladium nanowires is prepared with controlled Pt formation. These platinum and palladium nanowires that are resistive gas sensors have been used to detect hydrogen (H) gas in the air. The impact of the Pt surface layer was also evaluated [8]. In this research, the manufacture and characterization of hybrid structures (Al mesoPSi/AuPtPd-NPs n-Si/Al) as carbon monoxide (CO) gases sensors at room temperature have been reported. The hybrid metals in improving the performance of sensors and analyzing them on a large scale have been studied and analyzed.

## Experimental process

n-type Si (10  $\Omega$  cm and (100) orientation) wafers were used in this work. The Si wafers were cut into (3 cm  $\times$  3 cm) squares in size. Prior to etching, the native oxide was removed from the silicon wafers by immersing the samples in 1:10 mixture of 24% HF and 99.99% ethanol solution. Mesoporous silicon layers were fabricated by PECE using 1:1 mixture of 48% HF and 99.99% ethanol as the electrolyte. The silicon substrate and platinum cathode were kept perpendicular to each other at 0.6 cm separation, in a Teflon cell to form homogenous mesoPSi layers. The silicon substrates were etched by using a current density of (5 mA/cm<sup>2</sup>) for 30 min under (15 mW/cm<sup>2</sup>), 635-nm laser illuminations. In order to perform a good structural sensitivity assessment to the gas, the initial vacuum (0.2 mbar) was performed in the measuring chamber before the gas injection. HAuCl<sub>4</sub> (99.9%), HPtCl<sub>4</sub> (99.9%) and HPdCl<sub>4</sub> (99.99%) were attained from Sigma-Aldrich, Germany. HAuCl<sub>4</sub>, HPtCl<sub>4</sub> and HPdCl<sub>4</sub> solutions were prepared by dissolving in triply distilled water to create aqueous solutions of 6 mM. AuPtPd-NPs/mesoPSi heterostructures and bimetallic Pd–Ag NPs/macroPSi heterostructures were formed after dipping the porous layer interface into the chemical solutions for 10 min. Three chemical solutions (0.2 M HF: 6 mM HAuCl<sub>4</sub>), (0.2 M HF: 6 mM, HPtCl<sub>4</sub>) and (0.2 M HF: 6 mM HPdCl<sub>4</sub>/ HCl) were used for fabricating a mixture of both solutions AuPtPd-NPs/mesoPSi hybrid structures, respectively. The dipping deposition process of Au, Pt, and Pd on PSi layer occurs through the metal ion reduction process by the dangling bonds Si–H of the PSi according to the resulting anodic reaction. The immersing method was better than pulsed laser deposition (PLD) system and spray pyrolysis system, etc., because it is rapid, control, simple, and low-cost method and does not require the vacuum chamber. The reduction method of AuPtPd-NPs by the dangling bonds of the PSi layer was known by the following equations [7, 8]:



A thin layer of aluminum (Al) with high purity has been deposited to form a connecting pole with a thickness of about ~ 16 nm on a lower mesoPSi/n-Si surface of about ~ 30 nm, where a modern certified system is used. This deposition was performed using vacuum evaporation. The resulting AuPtPd-NPs/mesoPSi hybrid structures were finally washed with deionized water and dried with N<sub>2</sub> gas. The required volume of the water was calculated based on the following equation [4]:

$$\text{molarity} = \frac{w}{m_w} \times \frac{1000}{\text{voloum}} \quad (5)$$

where  $W$  the weight in g and  $m_w$  the molecular weight in g/mol. The front electrical contact above the AuPtPd-NPs/mesoPSi structures was fabricated by depositing a thin aluminum layer. Figure 1 illustrates a schematic diagram of the experiment of the AuPtPd-NPs embedded in the mesoPSi layer. Morphological characteristics of the AuPtPd-NPs and mesoPSi were studied using by scanning electron microscopy (SEM) image (JM-5600) fortified with an energy-dispersive X-ray diffraction (XRD) analysis device. The structural characteristics were studied by means of XRD-6000, Shiemadzu X-ray diffract meter. Hybrid samples were protected in a small sealed chamber at the CO gas pressure of 0.3, 0.9, and 2 mbar, respectively. Current–voltage characteristics were studied in darkness at room temperature by a fine DC power supply ad 8846 flukes 6-1/2 digit precision multi-meter.

## Results and discussion

The development of mesoporous silicon and modification with metal nanoparticles were done by the PECE method-fabricated mesoPSi layers. After formation, the mesoPSi substrates were rinsed with distilled water and allowed to dry the surrounding air.

Electromagnetism of these metallic is higher than PSi, and metal ions are thought to be in the mesoPSi surface circumference to capture-electrons of the PSi. The deposited metal atoms are formed first as nuclei forming nanoclusters to give nanoparticles. The noble metals (Au, Pt, and Pd) are on the surface of PSi toward sensing gas and result in high sensitivity at room temperature, while in metal oxide (e.g.,

**Fig. 1** Diagram of experiment Al/AuPtPd-NPs/mesoPSi/Si/Al hybrid structure

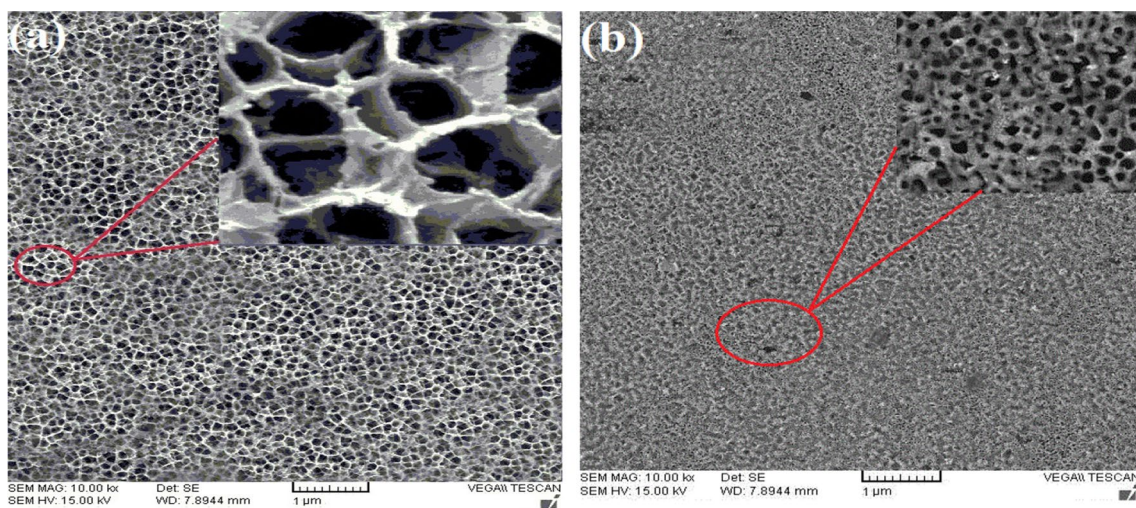
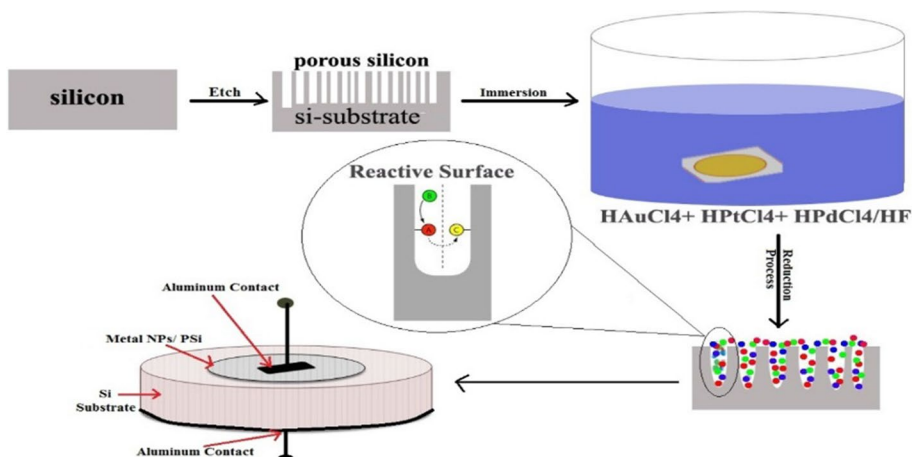


**Fig. 2** SEM images of **a** bare porous silicon and **b** AuPtPd-NPs/porous silicon

ZnO, TiO<sub>2</sub>, WO<sub>3</sub>, and SnO<sub>2</sub>) with great sensitivity, it mainly depends on the high working temperature, which is often achieved through a heated filament due to the temperature of the reaction O-. So, the noble metals in this work are better than the metal oxide [9]. Figure 2a shows a circular pore-like construction of uniform distribution over the surface. Mesopore-like structure which owns the peak pore sizes varying from 0.61 to 35.02 nm and the minimum pore sizes of about 100 nm is integrated by the Program ImageJ 8, from the surface morphology of mesoPSi layer before incorporating the AuPtPd-NPs. Figure 2b illustrates the SEM images of AuPtPd-NPs on the mesoPSi layer. Uniform particles inside the porous matrix are distributed with agglomerated AuPtPd-NPs particles that fully cover the silicon surface, with an average particle size of 0.64–7.53 nm.

The XRD patterns of the PSi-supporting Pd, Au, and Pt electro-catalysts are shown in Fig. 3 which shows that the XRD patterns of the AuPdPt/PSi are identical to those of the

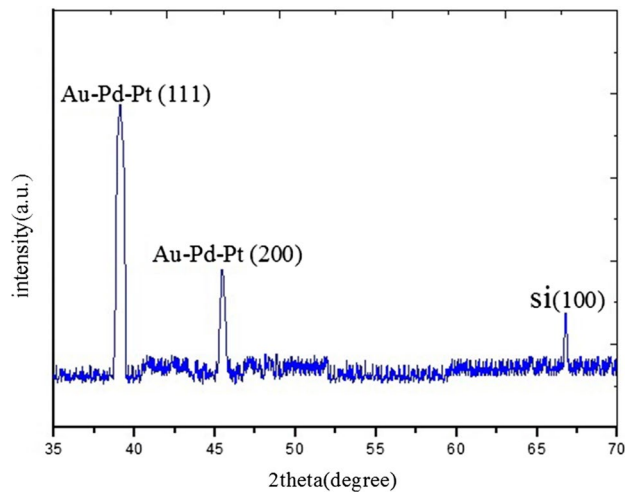


**Fig. 3** XPS spectra of Au Pd Pt/PSi for catalysts

hybrid structure. The resulting diffraction peaks located at  $2\theta$  values of  $39.12^\circ$ ,  $45.43^\circ$ , and  $66.78^\circ$  are attributed to the (111), (200), and (100) planes of AuPd, Pt, and PSi, respectively [8]. Another meaning of XRD is a strong method to determine the crystalline structure of crystalline material. By the diffraction pattern, XRD is used to determine particle size by Debye–Scherrer [10]:

$$D = 0.9\lambda/\beta \cos \theta \quad (6)$$

where  $D$  is the nanocrystal diameter, is the full width half maximum (FWHM) of the peak in radian,  $\theta$  is the Bragg angle, and  $\lambda$  = the wavelength of light. Figure 3 signifies XRD pattern for AuPd, Pt, and PSi. This size increases from the XRD peaks due to the small size of the granules due to the decrease in radiation individually. The slight variation in diffraction angle 2 can be observed. This variance is due to the existence of a local microscopic malformation (microscopic deformation, i.e., a local difference of interatomic distance of AuPdPt nanoparticles) of mesoPSi layers, referred to as a microstrain which is in a good agreement with results [8].

## Electrical characterization

Figure 4a, b illustrates the forward current–voltage characteristics ( $J$ – $V$ ) of the Al/mesoPSi/ $n$ -Si/Al structures with and without modification at room temperature. It can be seen from Fig. 4a that the current–voltage characteristics  $J$ – $V$  of as-formed PSi unmodified structures behave as an Ohmic contact at change pressures. Nevertheless, the effects of incorporating metal-NPs in a porous matrix on the current–voltage characterization ( $J$ – $V$ ) of Al/AuPtPd-NPs/mesoPSi/Al at room temperatures have been investigated. The AuPtPd-NPs deposition rectification properties improve when the forward current increases; this is due to Schottky contact structure and decreased resistance to porous layer. These effects show the barrier height of contact of metals, Si and Al with the PSi layer. It is noticed that for silicon  $n$ -type, the height of the barrier ( $\Phi_B$ ) is associated with the work function ( $\Phi_m$ ) via the equation [11–12]:

$$\Phi_{Bn} = Q_m - \chi_s \quad (7)$$

where  $\chi_s$  is the electron affinity. From Eq. (7), the work functions of Si and Al with the PSi layer can be concluded. This is in agreement with the literature. Indeed, the values of the work function of Al, Au, Pt, and Pd are 4.13 eV, 4.59 eV, 5.75 eV, and 4.92 eV, respectively. The forward  $I$ – $V$  characteristic of the Schottky barrier diode based on mesoPSi is that of contact metal/mesoPSi. For rectifying contact, it is supposed to owe to the thermal emission current and can be expressed as follows [12]:

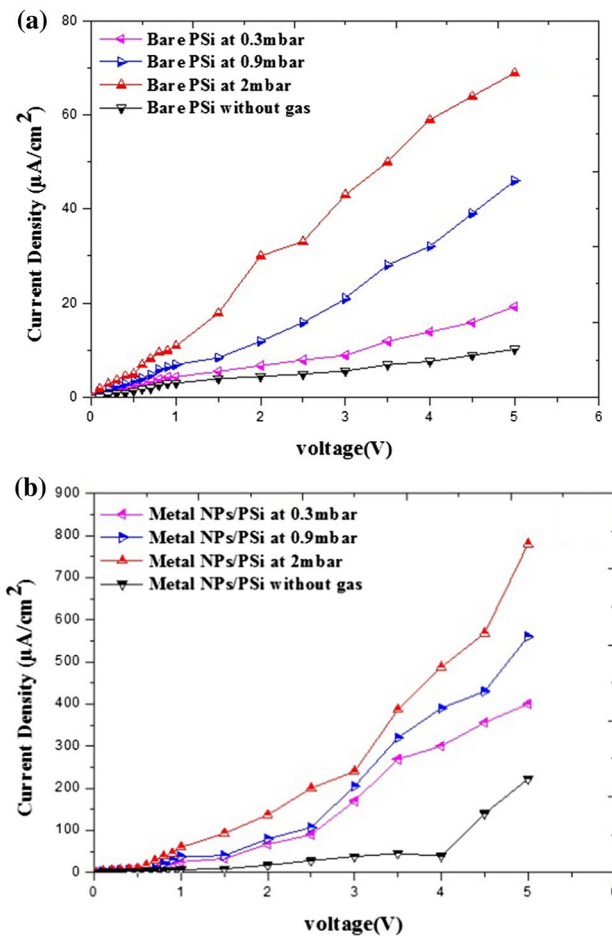


**Fig. 4** Forward  $J$ – $V$  characteristics of **a** as-formed mesoPSi and **b** metal-NPs-modified structures

$$I_{\text{Tot}} = I_0 \left[ e^{\left( \frac{qV}{nkT} \right)} - 1 \right] \quad (8)$$

$$J_0 = A^{**} T^2 e^{(-q\Phi_B/K_B T)} \quad (9)$$

where  $\Phi_B$  is the barrier height,  $I_0$  is the saturation current density,  $V$  is the applied voltage,  $A^{**}$  is the effective Richardson constant ( $112 \text{ A/cm}^2 \text{ K}^2$ ) for Si ( $n$ -type),  $T$  is the total temperature, and  $n$  is the ideality factor. The values of ideality factor ( $n > 1$ ) have been determined. On the other hand, it is difficult to directly determine the value of the barrier height  $\Phi_B$  by Eq. (9) for the reason that the definite value of the  $A^{**}$  for Schottky barrier diode based on mesoPSi must be well known. In fact, it is important to note that there are no reported values of Richardson constant  $A^{**}$  for Schottky barrier diode based on mesoPSi in agreement with [12].

Figure 4a, b illustrates the  $J$ – $V$  characteristics of Al/mesoPSi/ $n$ -Si/Al and Al/AuPtPd-NPs/mesoPSi/ $n$ -Si/Al structures sandwich as a function of variation voltage at

room temperature, respectively. All measurements have been taken in dark conditions ranging from 0 to 5 V. In Fig. 4a, the curves mesoPSi typically having rectifying behavior at the presence or absence of CO gas did not vary the shape of J–V characteristic of the linear J–V curve (Ohmic contacts), while in Fig. 4b, the deposition of AuPtPd-NPs has been noticed over or inside the mesoPSi layer on the electrical properties from manufacturing a gas sensor in the presence or absence of the CO gas [5, 13]. Based on the AuPtPd-NPs and mesoPSi, the gas senses behaviors in the presence of gas molecules, and the current increases by increasing the gas pressure as shown in Fig. 4a, b. The adsorption of the CO gas molecules has a significant effect on the J–V characteristics of the device. There are a number of approaches to clarify the increase in the current in the existence of CO gas this agrees with [14].

The dangling bonds formed with density in the porous silicon have resulted in the activation of the charge carriers which in turn lead to the enhancement and improvement of the variable connections of the charge carriers, and this agrees with [3, 10]. This variation is connected to the adsorption of the (CO) molecule on the porous silicon layer owing to the result of the van der Waals interaction. The CO desorption will lead to a change in the dielectric constant of the porous layer. The requirement of the dielectric  $\epsilon_{r\text{PSi}}$  on the porosity of the porous layer and the embedding medium ( $\epsilon_{r\text{pore}}$ ) is given by Eqs. (4–1).

$$\epsilon_{r\text{PSi}} = (1 - P\%)\epsilon_{r\text{si}}^{\frac{1}{3}} + P\%\epsilon_{r\text{pore}}^{\frac{1}{3}} \tag{10}$$

where  $P\%$  is the porosity of the porous layer and the  $\epsilon_{r\text{pore}}$  is the dielectric constant of the embedding medium (CO molecule). Furthermore, the AuPtPd-NPs deposited on the walls inside the silicon in the porous matrix act as additional sources to improve the surface area and hence enhance the gas adsorption rate. The forward current increases with increasing the deactivation process of the charge trapping centers (dangling bond) due to the existence of AuPtPd-NPs layer with high aggregation forms that agree with [3, 10]. The response time is well defined as the time necessary for the sensor to reach 67% of the total change for a given concentration of hydrogen, and the recovery time is well defined as the time needed to reach 67% of the total change after the hydrogen being cut off.

The relation response of current ( $S$ ) has been done using Eq. [3]:

$$S = \left| \frac{I_s - I_a}{I_a} \right| \tag{11}$$

where  $I_s$  and  $I_a$  are the current in the absence and presence of gas, respectively. The voltage–response characteristics are allowed for the determination of the range of the voltage

in which the response is ideal for different concentrations. Figure 5a, b shows the voltage–response characteristics of Al/mesoPSi/n-Si/Al and Al/AuPtPd-NPs/mesoPSi/n-Si/Al structures under three gases concentrations at room temperature. The relation response of the structures grows with gas molecules concentrations. The maximum response has been obtained for a sensor of AuPtPd-NPs as compared to mesoPSi. The highest sensitivity has been noticed at a bias voltage of about 0.1 V for AuPtPd-NPs compared to mesoPSi. It can be noted that the high response with modified structure was achieved for low biasing voltage for all structures, where it was a significant advantage that allowed the low power consumption to agree with [5].

The response time and recovery time characteristics of the samples were measured for three gas concentrations at room temperature. Figure 6 shows the passing response of Al/mesoPSi/n-Si/Al and Al/AuNPs/mesoPSi/n-Si/Al structures under three concentrations of CO (0.3, 0.9, and 2 mbar) at the optimum biasing voltage. Figure 6 shows

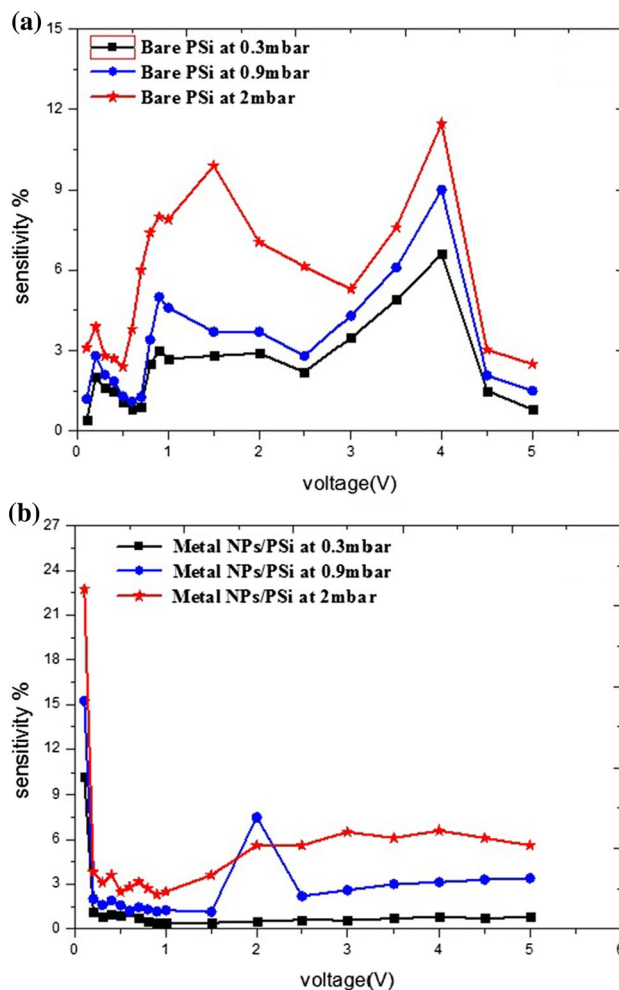
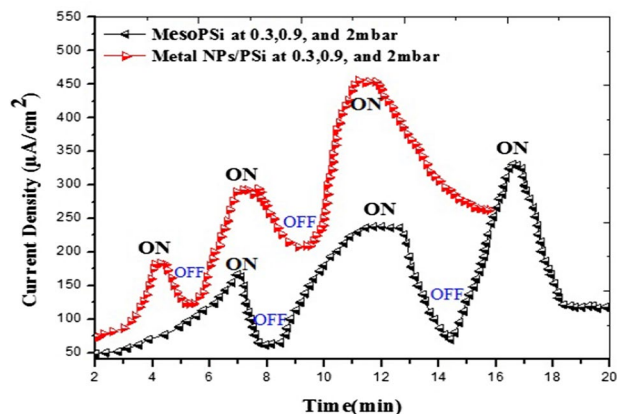


Fig. 5 Voltage–response characteristics of a as-formed mesoPSi and b AuPtPd-NPs-modified structures



**Fig. 6** Recovery and response time's characteristics at three concentrations 0.3, 0.9, and 2 mbar of as-formed mesoPSi and metal-NPs-adjusted structures

**Table 1** Recovery and response times of as-formed mesoPSi and AuPtPd-NPs adjusted structures

Samples	Concentrations					
	Response time (s)			Recovery time (s)		
	0.3 mbar	0.9 mbar	2 mbar	0.3 mbar	0.9 mbar	2 mbar
As-formed mesoPSi	37.8	45	49.8	107.4	48	63.6
AuPtPd-NPs	13.8	23.4	28.2	100.8	84	132

that the response increases with the gas concentration of all samples. The great response time and the recovery times or response of the prepared or structurally adjusted sample may be due to the high rate of gas desorption and adsorption agreement with [14].

Table 1 shows the recovery and response times of the adjusted samples. The lowest response times of 37.8, 45 and 49.8 s and recovery times of 107.4, 48 and 63.6 s were noticed for mesoPSi unmodified structure for gases concentrations, while the highest response times of 13.8, 23.4 and 28.2 s and recovery times of 100.8, 84 and 132 s were recorded for AuPtPd-NPs-adjusted structures for all gas concentrations.

## Conclusion

In this work, an easy and inexpensive technique has been constructed to fabricate gas sensing depending on mesoPSi synthesized with noble metals. Surface modification, after preparing the mesoPSi by PECE method, is carried out by

incorporating morphologies of AuPtPd-NPs. The simple immersion method of mesoPSi in different aqueous solutions of  $\text{HAuCl}_4 + \text{HPtCl}_4 + \text{HPdCl}_4/\text{HF}$  has been employed to synthesize AuPtPd-NPs. It has been observed that the sensor response depends greatly on the AuPtPd-nanoparticles. The minimum response and recovery times with the maximum sensitivity were achieved after depositing AuPtPd-nanoparticles. Incorporating noble metals such as Pt, Au, and Pd on the surface of mesoPSi can act as a good catalyst to adjust surface reactions of PSi toward sensing gas, resulting in high sensitivity. Thus, it can be used for manufacturing low-cost sensor methods on a chip and at a low power.

## References

- Gabouze, N., et al.:  $\text{CO}_2$  and  $\text{H}_2$  detection with a  $\text{CH}_x$ /porous silicon-based sensor. *Vacuum* **80**, 986–989 (2006)
- He, G., Narushima, T., Iguchi, Y., Goto, T., Hirai, T.: 11th International Conference on Solid-State Ionic, Waikiki Beach, Honolulu, Hawaii (1997)
- Alwan, A.M., Dheyab, A.B.: "Room temperature  $\text{CO}_2$  gas sensors of AuNPs/mesoPSi hybrid structures. *Appl. Nanosci.* **7**, 335–341 (2017)
- Alwan, A.M., et al.: Well controlling of plasmonic features of gold nanoparticles on macro porous silicon substrate by HF acid concentration. *Plasmonics* **13**, 2037–2045 (2018)
- Naama, et al.:  $\text{CO}_2$  gas sensor based on silicon nanowires modified with metal nanoparticles. *Mater. Sci. Semicond. Process.* **38**, 367–372 (2015)
- Itoh, T., et al.: Nonanal gas sensing properties of platinum, palladium, and gold-loaded tin oxide VOCs sensors. *Sensors Actuators B: Chem.* **187**, 135–141 (2013)
- Sari, W., et al.: Oxygen sensors based on screen printed platinum and palladium doped indium oxides. In: *Proceedings 1* (2017)
- Li, X., et al.: Catalytically activated palladium@platinum nanowires for accelerated hydrogen Gas VV detection. *ACS Nano* **9**, 3215–3225 (2015)
- Alwan, A.M., et al.: Study the characteristic of planer and sandwich PSi gas sensor (comparative study). *Silicon* **10**, 2527–2534 (2018)
- Alwan, A., et al.: Morphological and electrical properties of gold nanoparticles/macroporous silicon for  $\text{CO}_2$  gas. *Iraqi J. Sci.* **59**, 57–66 (2018)
- Henisch, H.K.: Metal-semiconductor Schottky barrier junctions and their applications. *Proc. IEEE* **74**, 894 (1986)
- Baba Ahmed, L., et al.:  $\text{H}_2$  sensing properties of modified silicon nanowires. *Prog. Nat. Sci.: Mater. Int.* **25**, 101–110 (2015)
- Sadr, S., et al.: Effect of gold electrode annealing on gas sensing properties of nano- and microstructures of macroporous silicon. *Indian J. Pure Appl. Phys.* **51**, 860–863 (2013)
- Alwan, A., et al.: Study of the influence of incorporation of gold nanoparticles on the modified porous silicon sensor for petroleum gas detection. *Eng. Technol. J.* **35**(8), 811–815 (2018)

**Publisher's Note** Springer Nature remains neutral with regard to jurisdictional claims in published maps and institutional affiliations.